EVIDENCE FOR A 17-YEAR CYCLE IN THE IMF DIRECTIONS AT 1 AU, IN SOLAR CORONAL HOLE VARIATIONS, AND IN PLANETARY MAGNETOSPHERIC MODULATIONS

DAVID A. JUCKETT
Barros Research Institute, 2430 College Rd. Holt, MI 48842, U.S.A. and Department of Chemistry, Michigan State University East Lansing, MI 48823, U.S.A.

(Received 15 April 1998; accepted 24 June 1998)

Abstract. A dominant 16–17 yr cycle was observed in the net exposure times of the Earth to Toward and Away field directions of the interplanetary magnetic field (IMF). A cycle of the same frequency and phase was observed in the polarity of the long-term hemispheric differences in coronal hole distributions. This was determined from north/south differences in average Fe XIV green line 'quiet' regions at high- and mid-latitudes. It is argued that the 17-yr cycle is a fundamental oscillation of coronal hole topology, which is transferred to Earth via variations in the neutral sheet. A comparison of the 17-yr cycle to the 22-yr Hale cycle indicated that they are not identical, but rather, can mix to form a 75-yr cycle plus a 9-yr cycle. Evidence for the 75-yr cycle existed in the Earth's net exposure times to fields from the solar North and South, and in the long-term imbalance of solar quiet regions between the northern and southern hemispheres. The 9-yr cycle was manifested in the mid- to low-latitude Fe XIV modulations and in solar wind velocity variations in the ecliptic. At Earth, evidence for a similar 17-yr cycle was observed in the horizontal magnetic field observations in a multitude of surface magnetic recording stations. In addition, the detection of a 17-yr cycle in the Huancayo neutron monitor cosmic ray series suggests that the effects of this cycle extend to the heliospheric boundaries. It is concluded that sufficient preliminary evidence exists to consider the hypothesis that the Sun contains a magnetic moment with an oscillatory cycle of 17 years.

1. Introduction

The oscillations of the Sun span minutes to centuries. Some of these are vibrational or magnetic modes, while others are activity cycles. The sunspot cycle is the benchmark activity cycle exhibiting a mean period of approximately 11 years throughout the last 150 years. It has been demonstrated that this is part of an overlapping extended cycle (Wilson *et al.*, 1988; Wilson, 1994) that begins every 11 years near the poles and progresses to lower latitudes over the course of 18 – 22 years. During the last half of this progression, sunspots are evident, whereas during the first half, active regions must be observed with such techniques as the Fe XIV emission in the corona. Overall, the 11-yr activity cycle may be considered a 'rectified' manifestation of the 22-yr polar magnetic inversion cycle (Hale cycle) with the greatest sunspot activity occurring at the time of inversion – during the time of greatest uncertainty in dipole direction. In dynamo models, both the inversion and the extended cycle are hypothesized to result from the differential winding of poloidal

Solar Physics **183:** 201–224, 1998.

magnetic field lines by the differential rotation bands in the solar convective zone (Babcock, 1961). In resonance models, either magnetic (Stenflo and Vogel, 1986) or torsional oscillations (Bracewell, 1988) lead to these phenomena.

The sunspot cycle – as measured over the last two centuries – appears at very regular intervals, especially when examined within narrow latitude ranges (see Appendix 2). The cycle intensities vary considerably however, and the historical sunspot record includes epochs of virtually no observable sunspots (e.g., Maunder, Spörer, and Wolf minima). For the dynamo or resonance theories to remain consistent with these activity dynamics it must be postulated that more than one cycle drives sunspot occurrence, such that their interactions lead to the amplitude modulations observed in the long-term sunspot activity (e.g., Sonett, 1983). These interacting cycles have not been definitively identified, but it seems likely that the Hale cycle will be a major component. Cyclical variations in a higher-order magnetic moment may provide a second interacting oscillation. This would be manifested in the topological dynamics of the open and closed magnetic regions of the solar outer layers.

While the short- and long-term dynamics of solar active regions have been extensively studied, the open-field regions of the Sun are less well understood. Even though mid-latitude coronal holes tend to compliment the active regions in both spatial distribution and time of occurrence (Dorotovic, 1996; Bravo and Steward, 1997), they don't necessarily follow either the same (or opposite) topological dynamics. Their complex behavior may be the result of oscillations in solar multi-pole magnetic fields (Stenflo and Vogel, 1986; Kundt, 1993), but a long-term description of this behavior is lacking.

After their verification and extensive study during the *Skylab* mission, progress has been made in understanding the short-term dynamics of coronal holes (Hoeksema, 1992; Richardson *et al.*, 1994; Wang and Sheeley, 1994; Erofeev, 1997; Storini *et al.*, 1997). This study represents an indirect exploration of their long-term dynamics and presents preliminary evidence that a 17-yr cycle is a major component in their behavior. A 17-yr cycle was detected in the long-term distribution of Away and Toward IMF at 1 AU, which is representative of the neutral line dynamics as transmitted to the interplanetary neutral sheet. This cycle correlates to an oscillation in the north/south difference in Fe XIV quiet regions in the solar corona, to horizontal magnetic field modulations at surface recording stations on Earth, and to high-rigidity galactic cosmic-ray modulation. The existence of the 17-yr cycle is further supported by the detection of 9- and 75-yr cycles, which are the predictable mixing products of the 17-yr cycle with the 22-yr Hale cycle. These products were observed in hemispheric imbalances of solar open field sources, the Earth's net exposure to magnetic fields from the two solar hemispheres, and in ecliptic solar wind variations. (Note: for simplicity, these cycles are referred to with the integers 17, 22, 9, and 75 although several estimates will be given that differ slightly from these values.)

2. Data Sources and Analysis

2.1. DATA

Inferred IMF directions, for 1947 – 1994, were obtained from the National Geophysical Data Center (NGDC), in electronic form. These data were provided by Stanford (originally compiled by Svalgaard), and by observatories in Vostok and Thule. The interplanetary magnetic field directions were derived from ground-based geomagnetic field observations near polar regions (Hirshberg and Colburn, 1969; Mansurov and Mansurova, 1970; Svalgaard, 1972). Additional data, covering the time from 1927 to 1972 was also obtained in tabulated form (Svalgaard, 1972).

Data for Fe XIV coronal green-line emission, at 530.3 nm, were obtained from the NGDC. The coronal intensities are given in millionths of intensity of the solar disk (coronal units) and converted to the photometrical scale of Lomnický Štít Station at a height of 40″ above the solar limb. Several stations were used in this database with Lomnický Peak being the primary station since 1965 (Rybanský *et al.*, 1994a; 1994b).

Horizontal terrestrial magnetic field measurements, for various surface recording stations, were obtained from the CD-ROM (Solar Variability Affecting Earth, NGDC 05/1). Annual horizontal field measurements at each site were used after detrending. Climax and Huancayo neutron monitor data was obtained from the same source and updated to 1997 by FTP electronic transfer from NGDC.

The yearly sunspot series ((Waldmeier, 1961), plus current years compiled by the NGDC), was smoothed with a 3-yr moving average. Data for sunspot groups was obtained from NGDC, as provided by Greenwich Observatory (1874 – 1981), Mt Wilson Observatory (1962 – 1989), and USAF (1988 – 1996).

Solar wind velocity data was obtained from the National Space Science Data Center (NSSDC) OMNIWeb data acquisition internet site. Hourly values spanning 1965 to the present were retrieved.

An estimate of the Hale cycle was obtained by inverting odd numbered solar sunspot cycles, represented as yearly average counts, smoothing the result and then raising each point along the curve to $\frac{1}{5}$th power. The resulting series was time shifted to coincide with observed magnetic reversals of the last few solar cycles (Webb, Davis, and McIntosh, 1984; Makarov and Sivaraman, 1989). This generated an approximate square-wave representation of the Hale cycle that served to track the polarity of the north solar field. An inversion of the curve served to track the polarity of the south solar field.

2.2. SPECTRAL ANALYSIS

Spectral analysis was primarily performed with the FRF (forward/reverse filtering) technique described in Appendix 1. This provided an estimate of spectral content as well as wave-trains for major frequency components. All FRF analyses were

performed on the autocorrelation of the series under study. Fourier analysis and maximum entropy spectral analysis (MESA) were performed using the fast Fourier transform (FFT) and Burg's method, respectively.

A moving-window cross-correlation method was used to compare the extracted 17-yr cycle with the Hale cycle. The procedure entailed calculating the cross-correlation between two time-aligned, short segments from the two curves. The value of the cross-correlation was assigned to the time value corresponding to the center of the window that defined each segment. The window was then moved point by point down the length of the curves.

Frequency selective wave-train extraction was accomplished with two methods: Fourier filtering; and, FRF filtering. The Fourier filtering method entailed removing unwanted FFT coefficients and then taking the inverse Fourier transform. A minimum of 4 coefficients were always retained to reduce bias in phase and frequency of the final wave-train. The FRF filtering method involved setting the center band-pass frequency of the Butterworth filter (see Appendix 1) to the desired wave-train frequency and then passing the time series through the filter in both directions (to eliminate filter-induced phase shifts). These two methods were routinely compared to validate each other.

3. Long-Term Variations in IMF Directions at 1 AU

The time-varying exposure of the Earth to the interplanetary magnetic field (IMF) is complex due to the warped nature of the neutral sheet in the Sun's equatorial plane. The Away and Toward field directions change several times during each solar rotation, with the passage of sector boundaries. The sources of the Away and Toward fields oscillate, in turn, with the Hale dipole cycle. When the Earth is in a fold that exposes it to a northern field, it could be in an Away field or a Toward field, depending on the dipole orientation. During a single 11-yr solar cycle, 300 to 600 sector boundary crossings may occur. The individual boundary crossings induce perturbations in the Earth's geomagnetic field leading to brief changes in such phenomena as aurora occurrence, galactic cosmic ray penetration, geomagnetic storms, ionospheric effects, and possible climate connections (Stern, 1962; Yoshida, Ogita, and Akasofu, 1971; Wilcox and Colburn, 1972; Wilcox and Scherrer, 1972; Page, 1983; Wilcox, Scherrer, and Hoeksema, 1983; Slavin, Jungman, and Smith, 1986; Dryer, 1987; Sakurai, 1987; Yukutake and Cain, 1987; Richardson *et al.*, 1994).

In addition to these relatively rapid changes in field exposures, long-term, repetitive epochs of excesses in field directions are of interest because they represent variations in the neutral sheet, and by inference, the neutral line. The neutral line, in turn, is controlled by the dynamics of coronal holes (Hansen, Sawyer, and Hansen, 1974; Howard and Koomen, 1974; Wilcox and Svalgaard, 1974; Bothmer and Schwenn, 1992; Hoeksema, 1992; Wang and Sheeley, 1994). A better understand-

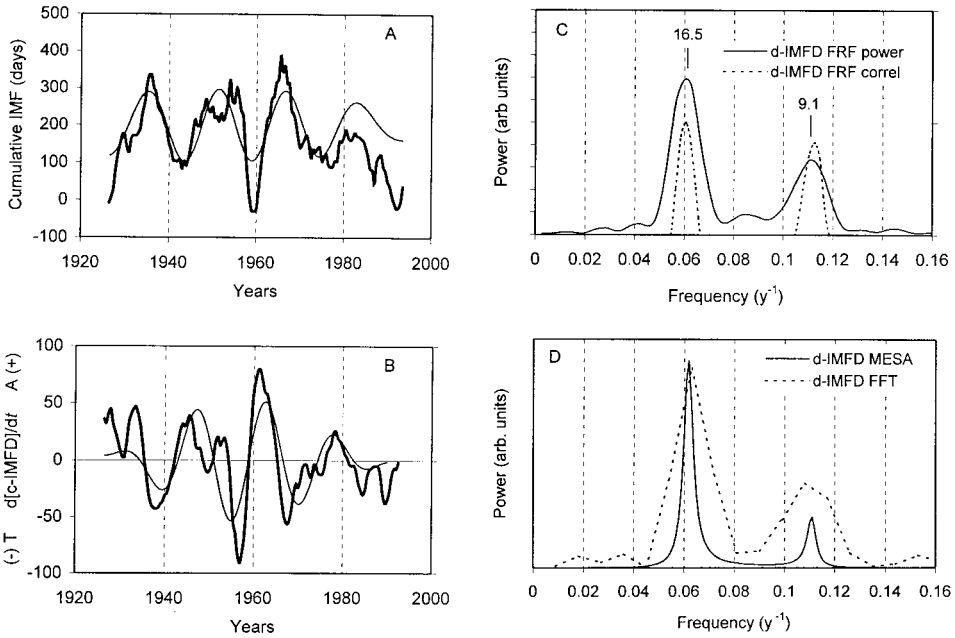

Figure 1. Calculation and analysis of c-IMFD and d-IMFD. (a) The cumulative IMF directions series (c-IMFD) constructed from an early series of Svalgaard, the Stanford series, and the Vostok series (see text). The 17-yr cycle, obtained by Fourier filtering, is shown by the light line. (b) The 1st derivative of the c-IMFD series in panel A was calculated numerically. The dominant frequency component is shown by the light line. (c) FRF spectral analysis (see Appendix I for method) of the d-IMFD autocorrelation series: power spectrum (solid); FRF correlation spectrum (dotted). Oscillation periods (in years) are displayed above spectral peaks. (d) Fourier analysis (FFT) and maximum entropy spectral analysis (MESA) of the d-IMFD autocorrelation series. For MESA: autocorrelation series length = 224, number of poles = 44.

ing of coronal hole dynamics, therefore, may be obtained by examining the long-term behavior of the neutral sheet, as detected by the Away and Toward field exposures at Earth.

An analysis of the IMF directions was performed using the IMF estimates available for every 24 hr. Following convention, the Away field was assigned a value of '+1', the Toward field a value of '−1', and an indeterminate direction a value of '0'. The running sum of these values, denoted c-IMFD, was computed for each data series, generating an 'integrated' version that was used for the subsequent analyses. The running sum and subsequent smoothing reduced the effects due to solar rotation and to the Earth's annual excursions above and below the solar equatorial plane.

A c-IMFD series was obtained for each of the 3 data sets, Stanford, Thule, and Vostok (see methods). A composite cumulative IMFD series was constructed from the concatenation of the Stanford and Vostok series. The much shorter Thule series tended to corroborate the Vostok series, but was not included. The daily series was

smoothed and sampled at time intervals of 0.5 yr. The earlier data (1927 – 1972) of Svalgaard had a disparate excess of Away days compared to the other sets, and no days listed as 'indeterminate'. This was corrected by incorporating a weighting factor for Away days equal to 0.88. This resulted in a cumulative series with no excessive Away trends and matched closely to the Stanford data in the overlap region. The older data was used to extend the Stanford data from 1947 backwards to 1927. The final composite series is shown in Figure 1(a).

To obtain a representation of the long-term excesses of Away and Toward field from the c-IMFD series, the first derivative was calculated numerically. The c-IMFD was initially smoothed with a moving average having a width of 3.5 yr (seven points), then the slope at each point was calculated. The resulting series was smoothed with a 1.5 year (three point) moving average. This is shown in Figure 1(b) and is referred to as the d-IMFD series.

The FRF analysis of the d-IMFD series is shown in Figure 1(c). The solid line represents the power profile and the dotted line represents the FRF correlation, which highlights the stationary components in the spectrum (see Appendix 1). The highest amplitude is associated with the 17-yr peak. A secondary oscillation has a period near 9.1 years. The numerical values of periods are shown above the peaks.

The MESA and FFT spectra for the d-IMFD series are shown in Figure 1(d). The Fourier analysis is not highly resolved because the shortness of the series results in poor resolution. The MESA spectrum is more highly resolved with the use of a sufficient number of poles. Typical of MESA on short series, however, the spectrum amplitude and identified frequencies were very sensitive to the number of poles used. In general, the results of the MESA and FFT spectra corroborate the major frequencies found in the FRF analysis and the concentration of power near the 15 – 17-yr region.

The d-IMFD series represents an alternation of the Earth's long-term, net exposure to IMF directions. This implies a 17-yr cycle in the average conformation of the neutral line, probably caused by imbalances in open field regions between the solar hemispheres. This 17-yr cycle in field direction is distinct from the magnetic inversion between the hemispheres (Hale cycle), as shown in Figure 2(a). These cycles indicate two separate processes that clearly move in and out of phase. The method of the moving-window correlation can be used to determine the average hemispheric sources of the excess IMF directions since the Hale cycle allows the association of polarity with hemisphere. When a Hale cycle curve is chosen so that it represents the oscillatory polarity of the north hemisphere, as in Figure 2(a), then positive correlations to d-IMFD indicate north hemisphere sourcing, while negative correlations indicate south hemisphere sourcing. The result of the moving correlation reveals a Gleissberg-type cycle (Figure 2(b)) in excess hemispheric field sourcing. An expansion of this cycle is shown in Figure 2(c), as obtained by mixing the 17-yr component of the d-IMFD series with a Hale cycle surrogate over a longer time span. (The hale cycle was represented by a sinusoidal function with a period of 21.4 yr (see Appendix 2) converted to a 'square wave' form by raising the values

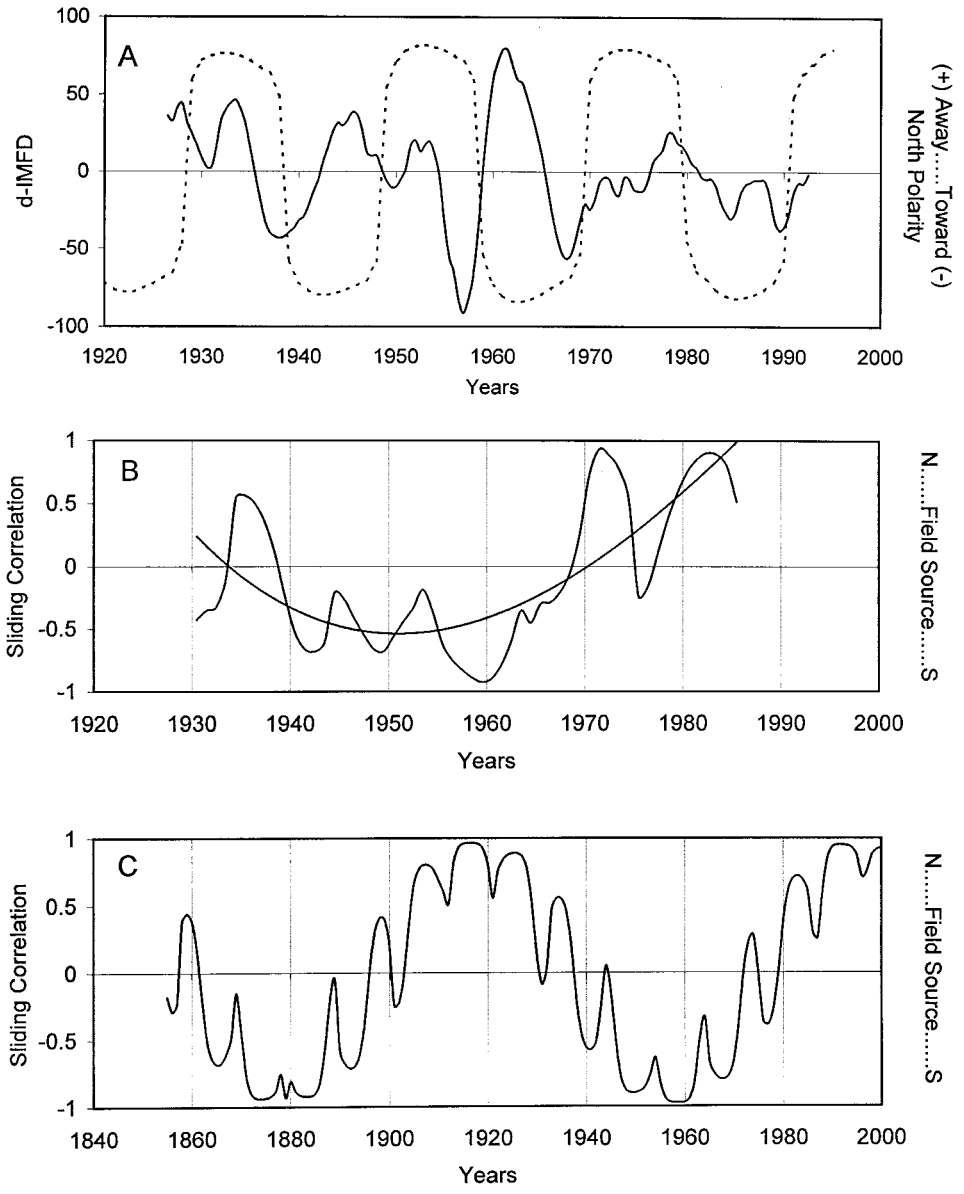

Figure 2. Assignment of solar hemisphere source locations to d-IMFD polarities. (a) The d-IMFD series of Figure 1(b) (solid) is shown with the northern hemisphere Hale cycle series (dashed). (b) Moving-window correlation of d-IMFD and Hale cycle using an 11-yr window. A 3rd-order polynomial fit (smooth line) represents the long-term trend. (c) A moving-window correlation between the Hale cycle surrogate (see text) and a cosine series with a period of 16.8 yr and phase angle chosen to synchronize to the 17-yr cycle of Figure 1(b). Note the longer period covered on the time axis compared to panels A and B.

to a power of 0.2). The 17-yr component was modeled with a sinusoidal function and was extrapolated back in time. The Gleissberg-type cycle indicates that the Earth is exposed to alternating excesses of fields sourcing from the southern and northern solar hemispheres with a repeat period of 75 years.

Also observable is a 9-yr cycle riding on this larger oscillation. These two cycles (9 and 75) originate from the 17- and 22-yr cycles because they are the sum and difference frequencies generated from non-linear mixing. The moving correlation method has the characteristics of a nonlinear operator that extracts these frequencies. The 9-yr ripple in Figure 2(c) indicates times when a sudden shift occurs towards sourcing from the opposite hemisphere. This effect is also consistent with the occurrence of isolated coronal holes, near the equator, bearing opposite polarity to the rest of the hemisphere. This interpretation is corroborated by synoptic maps of photospheric magnetic fields (e.g., Wang and Sheeley, 1994) and by the 9.1-yr oscillation also present in the d-IMFD series. This latter oscillation has the same phase as the cycle generated by the mixing of the 17- and 22-yr cycles (not shown) and would represent an additional modulation of the neutral sheet caused by these more equatorial coronal holes of opposite polarity.

4. Long-Term Variations in Coronal Hole Topology

The corona and coronal holes have been observed by several methods from Earth and from space platforms. The Fe XIV green-line emission has been correlated to active centers (Leroy and Noens, 1983), and synoptic maps of intensity have shown the progression of activity centers from the polar to equatorial regions (Altrock, 1992). Used in an opposite sense, the overall Fe XIV emission has been used to obtain a global estimate of the low-activity regions (Dorotovic, 1996; Bravo and Steward, 1997). Carrying this approach one step further, south/north imbalances can be determined from differences between the emissions in the individual hemispheres.

Daily Fe XIV green-line measurements were given for each of 72, five-deg regions, around the solar limb. The data base constituted 20 073 days spanning 1939 to 1994. The data was processed to obtain an estimate of long-term recurrent activity within a given latitude range. Specifically, the measurement from the western limb region of a given latitude range was averaged with the same latitude one rotation later (using latitude-specific rotation estimates to the nearest day). This, in turn, was averaged with the corresponding latitude range $\frac{1}{2}$ rotation away (averaged with its subsequent rotation), which was obtained from the eastern limb region of the same latitude. These daily values were obtained separately for the northern and southern hemispheres. Depending on the analysis, the northern values were either added to the southern values or were subtracted from the southern values. The resulting daily values were smoothed with a 151 day moving average. This series was then sampled every 150 days and then smoothed again by a seven-point

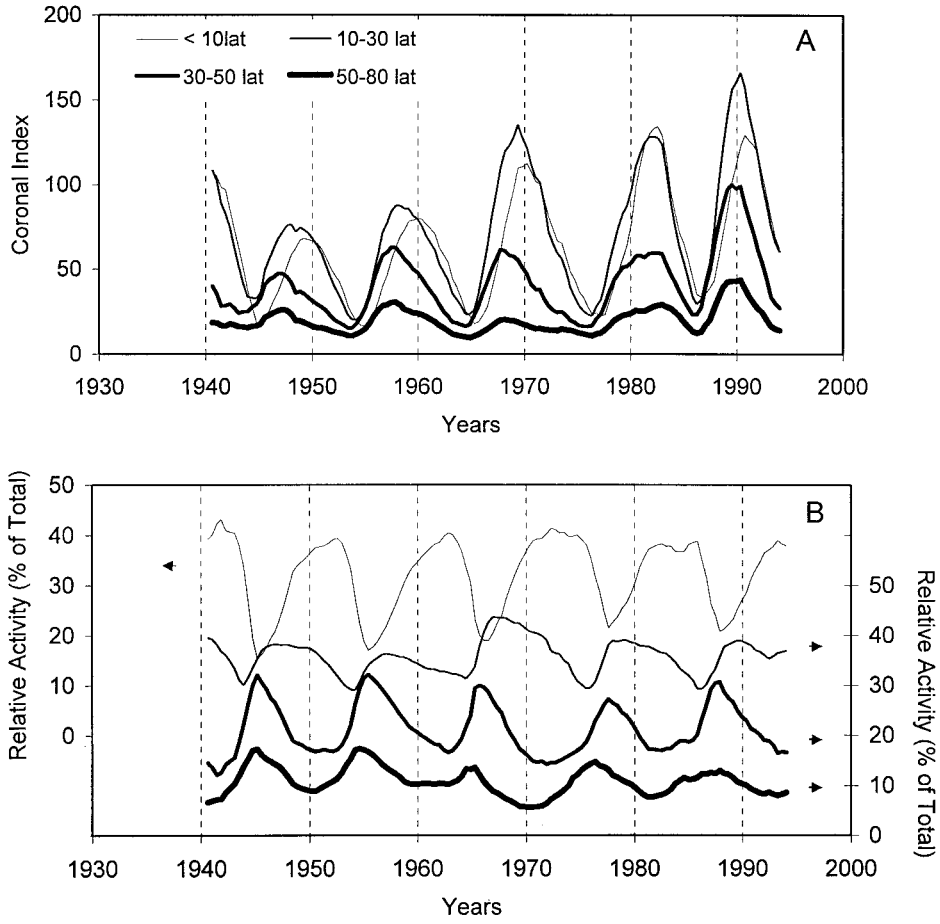

Figure 3. Coronal Fe XIV recurrent intensity and corresponding relative activity for four solar latitude ranges. (a) Average recurrent Fe XIV green line emissions for 4 latitude regions. The corresponding northern and southern regions were summed. A dominant 11-yr cycle exists for total solar activity at all latitudes. (b) The fractional contribution of each latitude region to the total activity was calculated at each time point. A clear progression occurs in relative activity from polar to equatorial regions. (The lowest latitude series is offset for clarity.)

moving average. The northern and southern series are referred to as C_n and C_s, respectively.

The method of averaging the recurrent Fe XIV activity over many rotations generated series indicative of the general, long-term activity within given latitude regions of the Sun. When the southern and northern series were summed, the resulting series exhibited the expected overall 11 year cycling of absolute activity as well as the progression of relative activity from polar to equatorial regions (Figures 3(a) and 3(b)). These southern and northern series were also used as estimates of the general, long-term behavior of the quiet regions by considering their inverses as

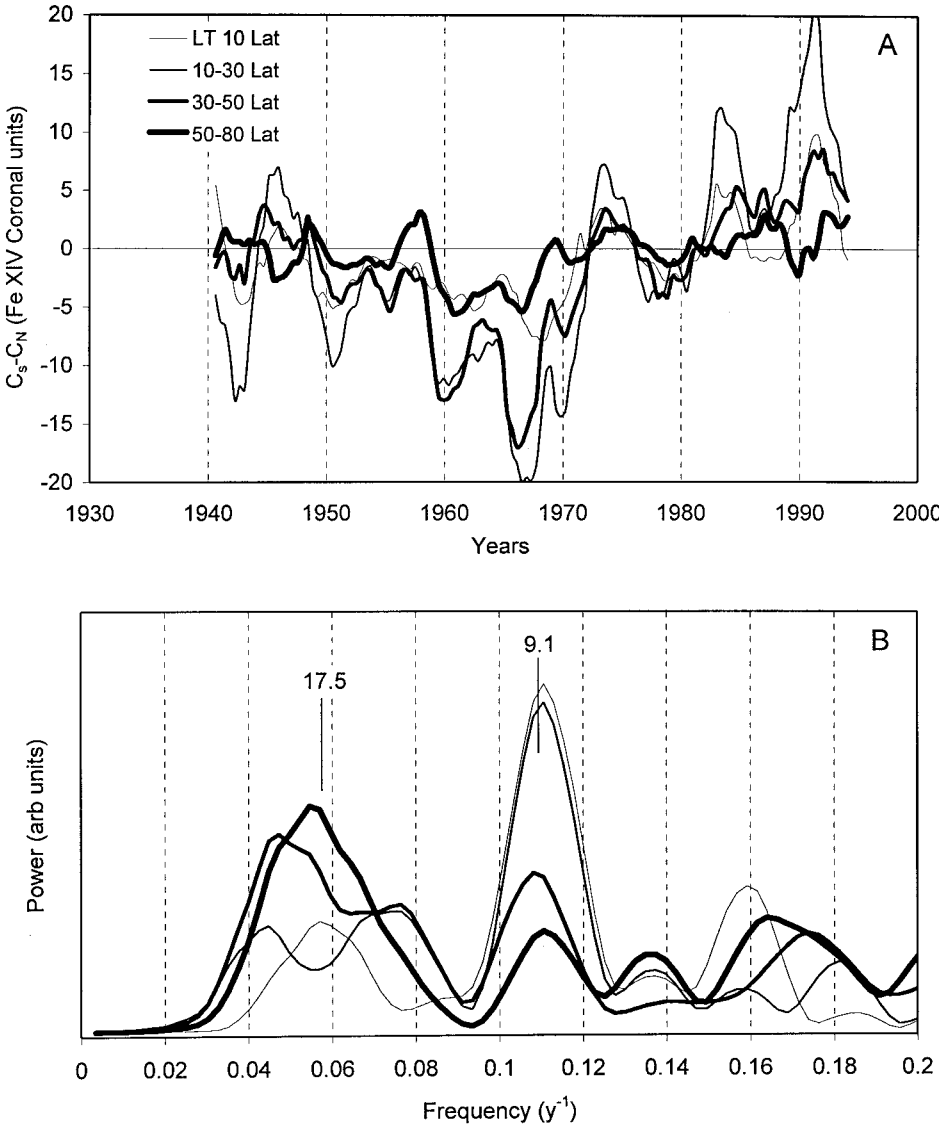

Figure 4. Solar hemisphere differences in coronal Fe XIV intensities and their spectral analyses. (a) The difference of the recurrent Fe XIV emission between the hemispheres is shown for the same latitude regions of Figure 3. By assigning low Fe XIV activity with high levels of 'quiet activity', then negative values of $C_S - C_N$ indicate excess quiet regions in the solar south, while positive values indicate excess quiet regions in the solar north (see text). (b) FRF spectra of the 4 series in (a). Before analysis the long-term trend was removed since periods longer than the times series cannot be determined accurately. A 9-yr cycle dominates the spectra for the two equatorial regions. Both 17- and 22-yr cycles appear more strongly at mid- and polar- latitudes.

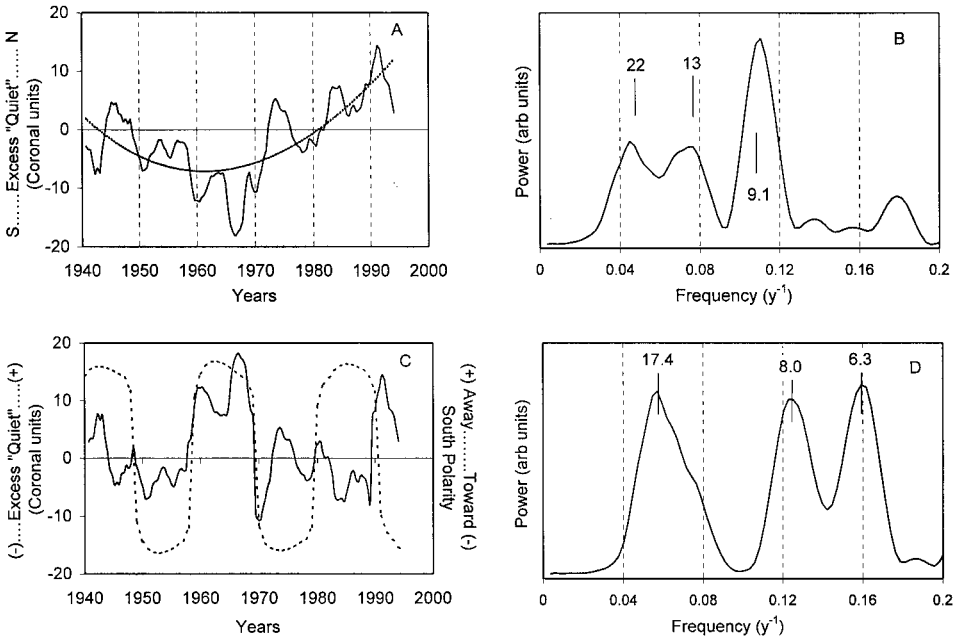

Figure 5. Solar hemisphere difference series in coronal Fe XIV intensities for the 10 – 50 deg latitude range, the assignment of polarity, and their spectral analysis. (a) The recurrent Fe XIV series for the latitude range 10 – 50 deg was used to calculate the hemisphere difference series. A 3rd-order polynomial fit is given by the smooth line. Positive and negative values are interpreted as in Figure 4(a). B) FRF spectrum of the Fe XIV coronal difference series of (a) after removal of the long-term trend. (c) Polarity was assigned to the series in (a) (solid) by inverting every half cycle along the Hale series (dotted). In this case the Hale cycle is given with reference to the South pole (opposite of Figure 2(a). The resulting series gives the trend in the polarity of the excess quiet regions. (d) FRF spectrum of the series in (c) with Fourier periods greater than 30 yr removed before analysis.

estimates of low activity. These series were then used to estimate the imbalance of low activity between the hemispheres. Such differences are shown in Figure 4(a). By taking the south-north difference of the Fe XIV recurrent activity (i.e., $C_s - C_n$), over a given latitude range, this is equivalent to $(-C_n) - (-C_s)$, were $-C_n$ and $-C_s$ represent estimates of low Fe XIV activity. Thus, positive values in the difference series represent an excess of low activity in the northern hemisphere, while negative numbers represent an excess of low activity in the southern hemisphere. The four different latitude ranges of Figure 4 indicate an apparent long-term oscillation between hemispheres. The series are not long enough to determine the full cycle, but the half-cycle is approximately 35 years long. The higher frequency components at these latitudes are shown in Figure 4(b). The long-term amplitudes were the largest for the two middle latitude ranges, so this wider range was analyzed further.

The south–north difference, in the Fe XIV intensity, for the latitudes spanning 10 to 50 deg is shown in Figure 5(a). This represents a slowly changing imbalance in quiet regions between the hemispheres. This long-term trend has the same char-

acteristics as the trend of Figure 2(b), which was obtained by removing polarity information to yield the hemispheric differences in IMF sourcing. The spectral analysis of this series (Figure 5(b)) also reveals a strong 9-yr cycle; similar to the secondary cycle obtained in Figure 2(c). When the polarity is incorporated into the coronal difference data, by inverting alternating Hale half cycles, then the 17-yr cycle becomes evident (Figure 5(c) and 5(d)). This makes it comparable to the d-IMFD series, which represents the polarity imbalance in the IMF. These two 17-yr cycles are virtually synchronous, which lends support for the interpretation that coronal hole imbalances lead to the imbalances in the IMF measured at 1 AU.

5. Further Evidence in Solar Wind Velocities

The 9-yr cycle is a particularly strong secondary oscillation in the d-IMFD cycle and in the Fe XIV coronal S – N series. In the latter case, this frequency appears to intensify toward the solar equator (see Figure 4(b)). Since coronal holes that extend to lower latitudes are usually associated with increases in solar wind velocities in the ecliptic (Hundhausen, 1977), a spectral analysis of solar wind was performed.

The daily solar wind velocity data was obtained for the years 1965 – 1995, smoothed, and sampled at half-year intervals. This is shown in Figure 6(a). The spectral analysis is shown in Figure 6(b) and shows a strong component with a period of 9.3 yr. Comparison of Figure 6(a) to the moving-window correlation of the 17-yr and 22-yr cycles, Figure 2(c), reveals a possible concordance of the solar wind increases with the regular deviations from the long-term trend in field sourcing. As commented earlier, these deviations may be consistent with isolated equatorial coronal holes, which would be likely to lead to higher wind speeds (e.g., Wilcox and Svalgaard, 1974; Howard and Koomen, 1974; Hoeksema, Wilcox, and Scherrer, 1982). The existence of this 9-yr cycle in the solar wind thus provides additional evidence for the existence of the 17-yr cycle coronal hole cycle and its non-linear interaction with the 22-yr dipole inversion cycle.

6. Earth Geomagnetic Variations Driven by d-IMFD

Earth-based magnetic recording stations have been used extensively to define several indexes of geomagnetic activity (Mayaud, 1980). These indexes are typically calculated by defining a magnetically quiet day each month and then determining deviations from this baseline. For such indexes as *Dst* and *Ae*, the horizontal field (*H*) measurements at the recording station are used. Measurements of *H* at mid- and equatorial latitudes give an estimate of the magnetospheric ring current (*Dst*), while measurements at polar sites give an estimate of the auroral electrojet current (*Ae*). Both of these indexes, however, are only sensitive to short-term changes in the magnetosphere since the subtraction of quiet day values removes long-term trends.

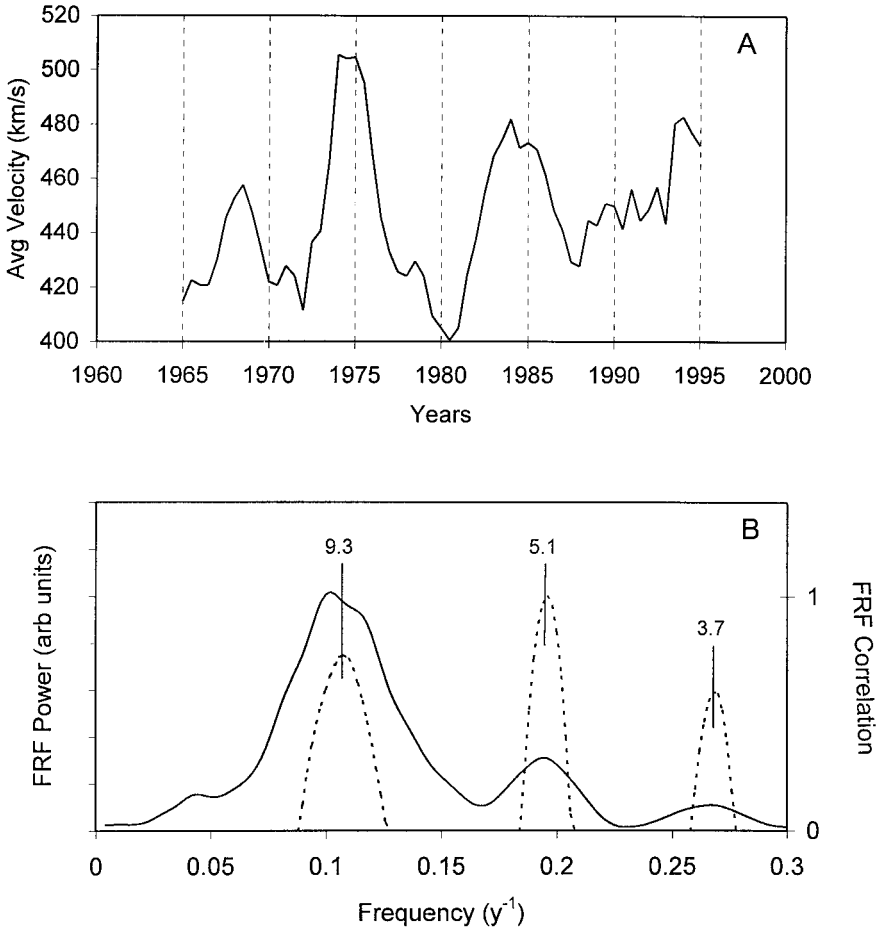

Figure 6. OMNI solar wind average velocity series and its spectral analysis. (a) Daily solar wind velocity measurements were smoothed and sampled at intervals of 0.5 years. (b) FRF power (solid) and FRF correlation (dotted) of the series in (a). The major power is near a period of 9.3 yr.

To examine possible magnetospheric effects from the long-term imbalances in IMF directions, the uncorrected *H* measurements were examined. Data from 25 recording stations, were used. Each had yearly estimates for more than 50 continuous years of operation. For each station, the secular trend and the frequency components having periods greater than 35 years, were removed by Fourier filtering. The resulting time series were normalized and the spectral content determined. Each station had an observable cycle with a period between 15 and 20 years. This is shown in Table I, along with the phase angle of the cycle and information on the recording station. The distribution of periods and phase angles for these stations are shown in Figures 7(a) and 7(b).

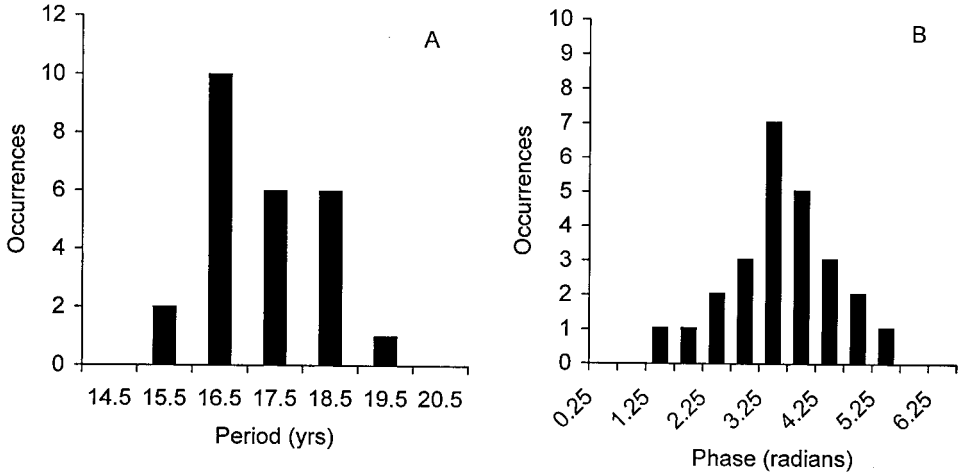

Figure 7. The distribution of observed cycle periods and phase angles for the 17-yr cycle in the horizontal magnetic field determinations at 25 Earth recording stations. (a) The distribution of periods for the 17-yr cycles observed in the recording stations shown in Table I. (b) The phase angle (with respect to the arbitrarily chosen phase = 0 at 1950) for the same set of stations.

For all the stations, the percentage of the total variance that is attributable to the 17-yr cycle, is less than 10%. This is primarily because the dominant, very long-term contributions to the horizontal magnetic field are expected to originate within the Earth's interior and, thus, would be stronger than those induced in the magnetosphere. Considering only those periods between 2 and 30 years however, the variance attributable to the 17-yr cycle is typically 30%. This is still a small change in the total field but is, nevertheless, comparable in absolute value to the disturbances (50 nT) used in the calculation of indexes such as *Dst* (Vennerstrom and Friis-Christensen, 1996). Due to the low overall intensity of the 17-yr cycle, 25 stations were examined to obtain a reasonable estimate of period and phase angle.

The average wave-train of the *H* 17-yr cycle is shown in Figure 8(a), together with 95% confidence limits. The numerical value of the average period and phase angle for the 25 stations is given in Table I. A model version of the oscillating IMF directions in the ecliptic is shown in Figure 8(b). This model was drawn to be compatible with the 17-yr cycle in the d-IMFD and the coronal S/N difference series (polarity added), as shown in Figures 8(c) and 8(d), respectively. Thus, there are wider (+) polarity pulses during times when d-IMFD exhibits excess Away field and the opposite for negative polarity times. Comparing to the *H* curve, the times of excess Away and Toward field are associated with the falling and rising *H* field, respectively. This indicates that the *H* cycle is 90 deg phase shifted with respect to the 17-yr cycle in the d-IMFD. This may imply that the pulse width variations in long-term Away and Toward field have an effect on the magnetospheric ring current. This could be interpreted as a slow rise in ring current (depressing *H*) during times of excess Away IMF field and a progressive drop in ring current

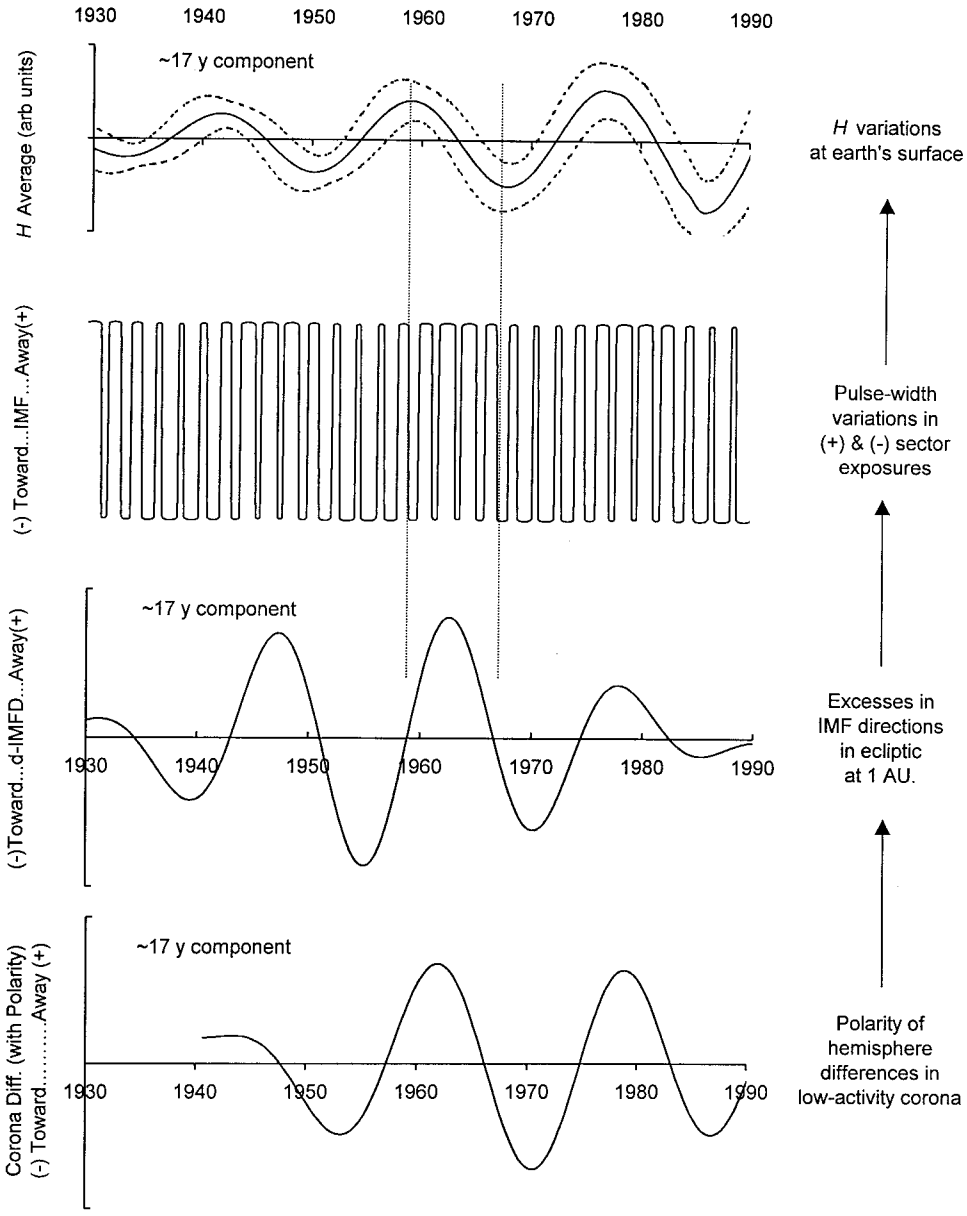

Figure 8. Compilation of observations on the 17-yr cycle from solar corona to IMF to the Earth's magnetosphere. The near synchrony of the 17-yr cycles from the imbalance in coronal quiet regions and the d-IMFD series (bottom two plots) is maintained for several decades. The pulse-width model of the IMF is meant to be indicative of the changes that are presumed to occur in the overall imbalance of Earth's exposure to Away and Toward sectors. The true number of sector boundaries cannot be drawn. The top panel represents the average of the 17-yr cycles from all 25 magnetic recording stations. The 95% confidence limits are given by the dotted lines.

TABLE I

Listing of magnetic recording stations together with the periods and phases of the 17-yr cycle in the observed horizontal magnetic field

Recording Station	Latitude (deg)	Longitude (deg)	Range (yr)		Length (yr)	Period (rad)	Phase
Apia	−13.81	188.23	1905	1988	83	17.86	1.41
Cheltenham	38.73	283.16	1901	1956	55	16.53	3.21
Coimbra	40.21	351.58	1866	1989	123	16.40	4.18
Dombas	62.08	9.10	1916	1987	71	19.00	2.90
Eskdalemuir	55.32	356.80	1909	1989	80	17.24	2.07
Honolulu	21.32	201.94	1902	1988	86	19.61	2.94
Kakoika	36.23	140.19	1913	1988	75	16.95	0.69
Lerwick	60.13	358.82	1923	1988	65	18.52	2.85
Lovo	59.35	17.83	1928	1988	60	17.24	2.04
Meanook	54.62	246.67	1916	1988	72	18.10	3.81
Niemegk	52.07	12.68	1931	1988	57	16.39	1.74
Pilar	−31.67	296.12	1905	1983	78	17.86	3.50
Rude Skov	55.84	12.46	1891	1984	93	18.86	2.95
San Fernando	36.46	353.80	1891	1979	88	16.00	0.48
San Juan	18.38	293.88	1926	1988	62	15.75	3.00
San Miquel	37.77	334.35	1915	1978	63	16.95	3.06
Sitka	57.05	224.67	1891	1979	88	16.67	2.37
Swider	52.12	21.25	1921	1972	51	16.95	3.86
Teoloyucan	19.75	260.82	1922	1977	55	16.30	4.43
Toolangi	−37.53	145.47	1919	1979	60	17.24	4.81
Tromso	69.66	18.95	1930	1988	58	16.67	1.54
Tuscon	32.25	249.17	1910	1988	78	17.70	3.91
Valentia	51.93	349.75	1899	1989	90	16.81	2.93
Vassouras	−22.40	316.35	1919	1988	69	18.50	3.31
Zaymishche	55.83	48.85	1912	1974	62	15.62	2.76
Mean						*17.27*	*2.83*
Std. Dev.						*1.05*	*1.10*

(increasing H) during excess Toward IMF field exposure. The mechanism of this effect is not obvious, however. It may be linked to a differential efficiency of Away and Toward field merging with the magnetosphere or with reconnection in the geomagnetic tail. Field-aligned currents inducing helical components may introduce different degrees of southward field components between Away and Toward field lines, thus generating a difference in field merging efficiency at the magnetopause.

Ultimately, however, more work must be done to determine if the 17-yr cycle in the magnetosphere is related to the similar period cycles in the d-IMFD and in coronal hole topology. If the relationship is validated, then the mechanism must be elucidated.

7. A 17-yr Cycle in a High-Rigidity Neutron Monitor

The 17-yr cycle in the d-IMFD and in the topology of solar open field structures predicts a heliospheric-wide effect that should contribute to the modulation of galactic cosmic rays (GCR) entering the heliosphere. To explore this, the spectral analyses of Climax and Huancayo neutron monitors are shown in Figure 9(a). There is a discernible cycle near 17 years in the Huancayo series, which is not readily detectable in the Climax series. All the remaining spectral features are virtually identical. To determine if the presence of this weak oscillation was an artifact of the spectral analysis, the difference series between the two sites was first calculated (see figure legend, Figure 9(b)) and then the spectral analysis was performed. The FRF spectrum of the difference series, Figure 9(b), yields a dominant 17-yr cycle.

The presence of the 17-yr cycle at the high rigidity site suggests that a 17-yr modulation of GCR extends to higher primary energies than the other modulating oscillations. Thus, at high rigidity sites, the 17-yr cycle would be a larger fraction of the oscillatory power since fewer of the low energy GCR penetrate the magnetosphere. At lower rigidity sites the lower energy primaries, dominated by the other frequencies, would overwhelm the 17-yr cycle.

An alternate explanation for the 17-yr cycle in the Huancayo series is a strictly local effect on the GCR flux through the oscillation in the *H* magnetospheric field. This seems improbable because all neutron monitors should exhibit similar traces of this cycle. In fact, Deep River, Canada, and Mt. Washington, U.S.A. neutron monitors show less 17-yr signal power than Climax (not shown).

The 17-yr cycle in the Huancayo neutron monitor is consistent with the detection of a similar cycle in the terrestrial Δ^{14}C record (Sonett, 1997), using the yearly data record of the Pacific Northwest pines (Stuiver, 1993). This cycle had come to the attention of Sonett several years ago (personal communication), but its connection to other processes was lacking. The existence of a 17-yr cycle in solar processes may allow further insight into the origins of this Δ^{14}C component. (See Sonett, 1998, submitted to *Solar Physics*, for further discussion.)

8. Discussion

8.1. SUMMARY

The telltale signature of a 17-yr cycle was observed in the directions of the IMF at 1 AU and in the polarity of coronal quiet region imbalances – using Fe XIV coronal

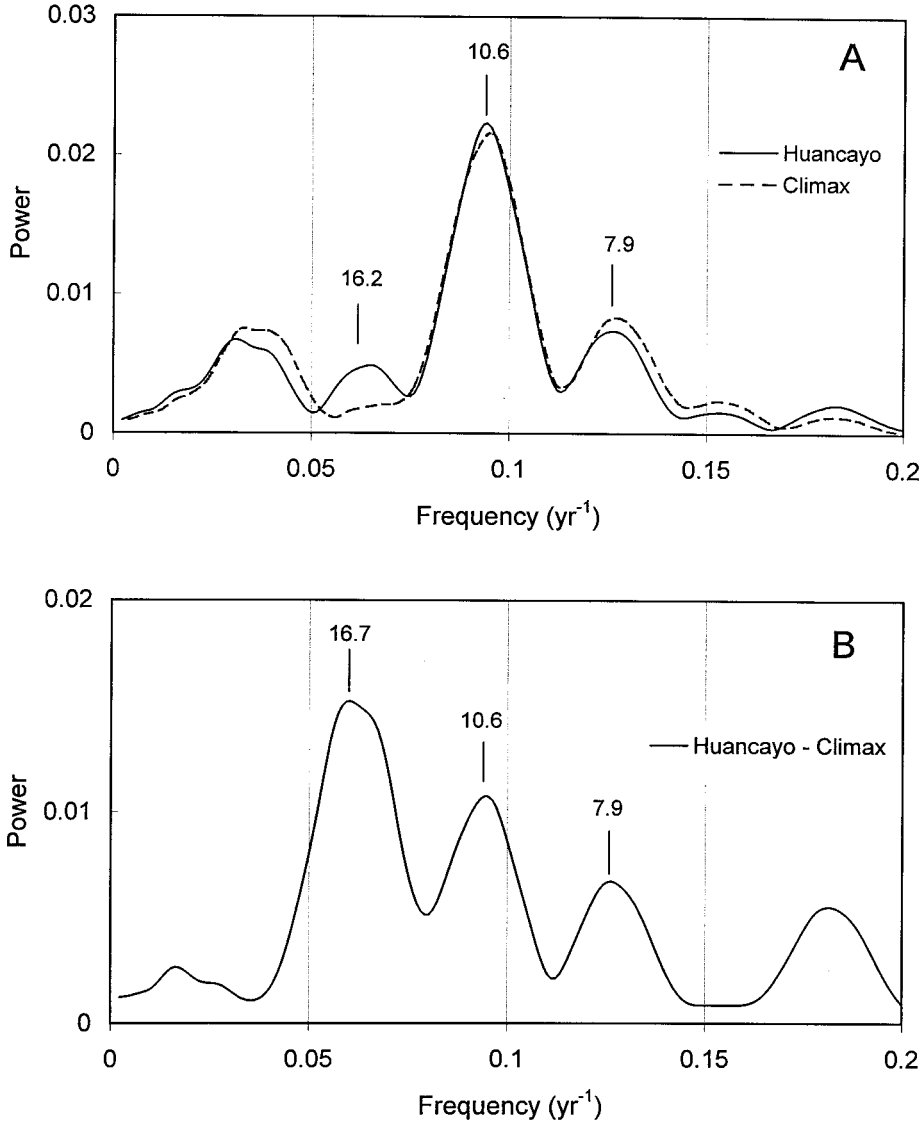

Figure 9. (a) Spectral analysis of Climax and Huancayo neutron monitor series. Both series spanned the years 1953 to 1996. Each was processed by FRF analysis and the resulting spectrum normalized to an area of 1.0. The periods (in yr) of major components are indicated above the peaks. The lowest frequency peak, below 0.05, is unreliable due to series length. (b) The FRF spectrum of the optimized Huancayo – Climax difference series. The difference series was calculated and its mean variance was minimized by scaling the normalized Huancayo series with respect to the normalized Climax series. The resulting series was smoothed with a 3-yr moving average and subjected to spectral analysis.

green-line intensity differences between the hemispheres. A long-term imbalance of the Earth's exposure to solar south and north field sourcing was also detected by using a moving-window correlation technique on the 17-yr d-IMFD cycle and Hale cycle. This generated a cycle of 75 years that was concordant with the general hemisphere imbalances in the coronal quiet regions. The moving-window correlation also elaborated a 9-yr cycle, which was shown to be similar to the solar wind velocity changes in the ecliptic.

The d-IMFD series contains information on both field source and polarity of the IMF, whereas the Fe XIV difference series contains source information only. When the d-IMFD series was converted to source-only information, by moving correlation to the Hale cycle, it had long-term time behavior consistent with the Fe XIV series. Similarly, when polarity was added to the Fe XIV difference series, it contained a 17-yr cycle that was consistent with the d-IMFD series. It seems reasonable to conclude, therefore, that these two phenomena are locked together by a cause-and-effect relationship.

The long-term horizontal magnetic field changes detected at 25 Earth-based recording stations also revealed a 17-yr cycle with average phase that was shifted $\frac{1}{4}$ wavelength from the coronal and d-IMFD cycles. The mechanism for this magnetospheric effect is not clear, however, there appears to be a phenomenological progression from Sun to interplanetary space to Earth.

Additional evidence for the 17-yr cycle was also seen in the high-rigidity Huancayo neutron monitor time series but its absence in the Climax monitor indicates its role in GCR modulation will need further work for clarification.

8.2. Additional comments

The 17-yr cycle, although quite pronounced in the d-IMFD series, has not been reported in the analyses of solar magnetic source fields. The spherical harmonic analyses of Stenflo and Vogel (1986) and Gokhale and Javaraiah (1992) have observed only the 22-yr cycle. This is partly due to the inability to distinguish these two closely spaced frequencies. Another reason for not detecting this cycle is that the 17-yr oscillation should be weak in the spherical harmonics of the zonal modes ($m = 0$), which were the only ones reported by these authors. Although the 17-yr cycle in d-IMFD implies an imbalance of the neutral line between hemispheres, the neutral line does not have the longitudinal symmetry expected for $m = 0$ modes. Rather, the neutral line has the general appearance of lying along select nodal lines of harmonics with $m > 0$. Therefore, evidence for the 17-yr cycle may be obtainable from one of the $m > 0$ harmonic components.

The 17-yr cycle in the d-IMFD appears to be synchronous with the 17-yr cycle detected by Smith and Beiber (1996) for the difference in helicity for Away and Toward sectors. Their analysis only covers approximately $1\frac{1}{2}$ cycles but the results are generally concordant with the observations reported above. Their deduction of a persistent south excess in helicity may result from the limited span of years in

their analysis, which coincides with only a portion of the 75-yr cycle in N/S IMFD excesses (Figure 2) and the N/S excesses in coronal quiet regions (Figure 5).

Using the Earth's geomagnetic indices as indicators of solar activity, Legrand and Simon have developed extensive evidence for a two-component model of the solar cycle (Legrand and Simon, 1991; Simon and Legrand, 1992). They suggest toroidal and poloidal cycles that are phase-shifted by approximately 5 years. These cycles appear to be two parts of the overall 22-yr (11-yr) magnetic cycle, and it is not clear if the 17-yr cycle is part of the phenomenon they observe. It seems possible that the dipole/multipole inter-modulations, which they consider part of the poloidal dynamics, may result from the interaction of 22-yr and 17-yr cycles. Further work in this regard is warranted.

The analysis of the north-south Fe XIV quiet region data required the addition of polarity (using a Hale cycle reference) in order to be comparable to the d-IMFD series and to yield the robust 17-yr cycle (Figure 5(d)). The addition of polarity also introduced 8.0- and 6.3-yr cycles. The analysis of these cycles (and whether or not they are artifacts) is beyond the scope of this article, but it is noted that the 17-yr and 8-yr bands in Figure 5(d) are identical in frequency to the two major sidebands of the neutron monitor spectra (Figure 9(a)). The complex oscillations of solar open field structures may leave their trace on GCR entering the heliosphere.

8.3. Conclusion

While the origin of the 17-yr cycle and its role in solar dynamics is not clear at this time, there is preliminary evidence for its presence in the distributions of coronal magnetic quiet regions, in interplanetary magnetic field dynamics, and in the Earth's magnetosphere modulations. In addition, indirect evidence for a 17-yr cycle has been observed (in the form of 9-yr and 75-yr cycles) in various aspects of field sourcing and solar wind parameters. Thus, the following hypothesis is presented for consideration.

> In addition to the solar magnetic dipole-inversion cycle (22-yr period), a major magnetic cycle with a period of 17 yr is also present in the Sun. This cycle, which is manifested in the distribution of open magnetic field structures and the asymmetry of the neutral line, may represent an independently oscillating solar magnetic moment.

Appendix 1

A Forward/Reversed Filtering (FRF) approach to spectral analysis and wave-train extraction is described. The method was developed to identify and extract oscillatory components using digital filtering methodologies. In the standard periodogram analysis or Fourier type analysis, rigid sinusoidal wave-forms (either orthogonal or non-orthogonal sets) are fit to the data to determine the signal variance of each

wave-form. As a simple alternative, FRF uses filtering techniques to extract estimates of the component wave-trains within the series. Such a methodology is not limited to constant amplitude sinusoids and can accommodate minor variations in both phase and frequency. FRF is less ambiguous than MESA (Maximum Entropy Spectral Analysis) in determining frequency values, and gives wave-train amplitude or power directly.

The FRF method is based on the digital filtering of time series (or their autocorrelation) in time-reversed and time forward directions. This bi-directional filtering extracts wave-trains as well as identifies dominant frequency components depending on how it is implemented.

The identification of frequency components is based on the non-linear phase shift behavior of IIR (Infinite Impulse Response) digital band-pass filters. In general, a non-linear phase response is an awkward byproduct of IIR digital filters. and must be corrected to avoid unwanted behavior (Rabiner and Gold, 1975; Stearns and David, 1988). Alternatively, the phase shift property of narrow band-pass filters can be used to discriminate between stationary frequency components and spurious oscillations. Narrow band-pass IIR filters exhibit a phase shift of zero only at the frequency where the gain is maximum. On the low frequency side of the maximum, the phase shift rapidly approaches a plateau having a value of ($\pi/2\times$ [filter order of high-pass section]), while on the high frequency side the phase shift approaches ($-\pi/2\times$ [filter order of low-pass section]). This property causes an oscillation to be phase-shifted at the filter output unless its characteristic frequency is exactly at the band-pass maximum.

For a filter order of one (for both the high-pass and low-pass sections of the band-pass filter) the correlation of the separate forward and reverse filter outputs identifies the off-center and on-center frequencies because of their opposite phase shifts. The correlation of the forward and reverse filter outputs for an off-center frequency will approach -1.0 because the outputs will be 180 deg out-of-phase. A strong positive correlation will occur only for time series containing oscillatory power at the band-pass center, where the phase shifts are zero.

FRF analysis is implemented with 500 filter settings, evenly spaced across the Nyquist frequency interval. The FRF correlation spectrum represents the correlation for forward and reverse filter passes at each frequency, with negative correlation values truncated to zero. This spectrum is useful for identifying stationary components of the time series.

To determine spectral amplitude or power, as well as extract wave-trains, a different implementation of filtering is employed. A method of Rabiner and Gold, (1975) is used, which yields filtered outputs containing no phase shifts. The method consists of: reversing the series; filtering; time reversing again; and, then filtering again. This corrects any phase shifts caused by the filter. The output of this procedure generates a wave-train suitable for identifying phase and for comparison to other wave-trains. The RMS (root mean squared) amplitudes of all the wave-trains constitutes an amplitude spectrum for the original time series. If the autocorrelation

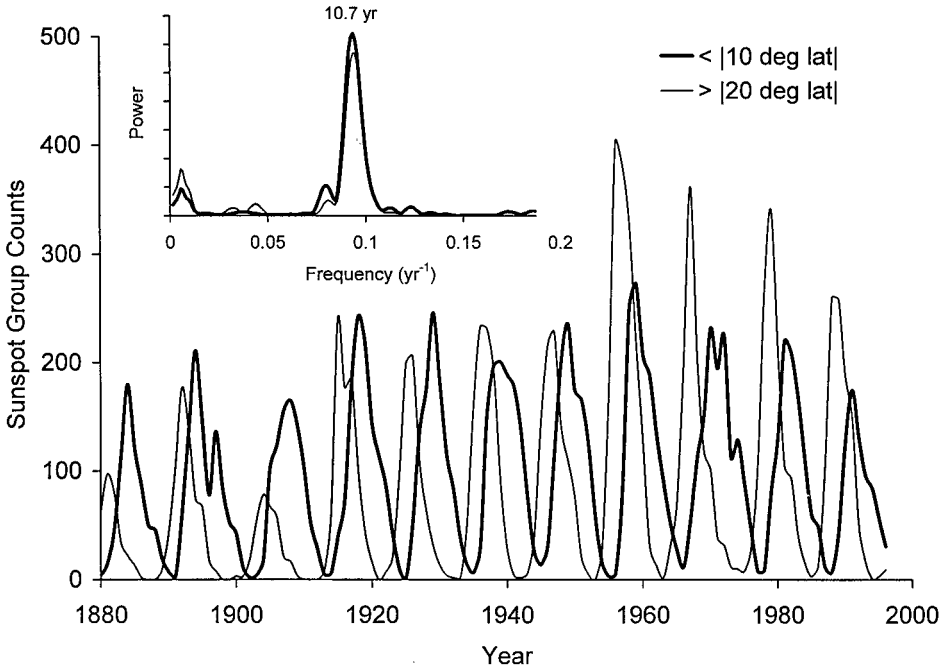

Figure 10. Distribution of sunspot group counts from two solar latitude regions. Two series were constructed from sunspot group counts. One series included only those groups with solar latitude between +10 and −10 deg (heavy line). The other series included only groups with latitudes greater than |20| deg (light line). The mid-latitude series precedes the equatorial series as would be predicted by the sunspot butterfly distribution. Spectral analysis (FRF) of these two sunspot group series is shown in the insert.

series is first generated for each series, then the normalized amplitude of the resulting wave-trains represents the power spectrum, since the autocorrelation 'squares' the original series.

The general implementation of the FRF method uses Butterworth IIR filters with bandpass width of $0.2/N$, where N is the series length. (This width is in units of sampling frequency.)

Appendix 2

The Wolf sunspot series, as usually depicted, represents spots observed at all latitudes. Part of the complexity and non-symmetrical shape of the individual cycles is a direct result of this concatenation across latitudes. By using sunspot groups, sorted by latitude ranges, a clearer picture of cycling emerges. As seen in Figure 10, time series constructed from two different latitude ranges show more symmetrical shapes and have fewer frequency components by spectral analysis (see insert, Figure 10). The more equatorial series (heavy line) has nearly uniform peak heights

across a time when the Wolf series changes by a least a factor of 2. Thus, the irregularity appears to stem from the variability in the occurrence of the higher latitude sunspots (which is where the 17-yr cycle is also strongest).

The strongly dominant period of the low latitude series is 10.7 yr. The same period is also dominant for the higher-latitude series, and for the series for the latitudes in between 10 and 20 deg (not shown). Doubling this value gives an estimate of 21.4 yr for the Hale cycle period. This coincides with the value obtained from spherical harmonic Fourier analysis of solar magnetic fields (Gokhale and Javaraiah, 1992) and was used in mixing calculations with the 17-yr cycle.

Acknowledgements

I am grateful for the support and encouragement of Dr Barnett Rosenberg. I also thank Dr Charles Sonett for valuable correspondence during the final stages of this paper. This work was supported by a joint research agreement between Barros Research Institute and Michigan State University.

References

Altrock, R. C.: 1992, *Bull. Am. Astron. Soc.* **24,** 746.
Babcock, H. W.: 1961, *Astrophys. J.* **133,** 572.
Bothmer, V. and Schwenn, R.: 1992, in E. Marsch and R. Schwenn (eds.), *Solar Wind Seven,* p. 151, Oxford, Pergamon Press, Ltd.
Bracewell, R. N.: 1988, *Solar Phys.* **117,** 261.
Bravo, S. and Steward, G. A.: 1997, *Solar Phys.* **173,** 193.
Dorotovic, I.: 1996, *Solar Phys.* **167,** 419.
Dryer: 1987, in S.-I. Akasofu and Y. Kamide (eds.), *The Solar Wind and the Earth*, Terra Scientific Publishing Co., Tokyo, p. 19.
Erofeev, D. V.: 1997, *Solar Phys.* **175,** 45.
Gokhale, M. H. and Javaraiah, J.: 1992, *Solar Phys.* **138,** 399.
Hansen, S. F., Sawyer, C., and Hansen, R. T.: 1974, *Geophys. Res. Letters* **1,** 13.
Hirshberg, J. and Colburn, D. S.: 1969, *Planetary Space Sci.* **17,** 1183.
Hoeksema, J. T.: 1992, in E. Marsch and R. Schwenn (eds.), *Solar Wind Seven*, Pergamon Press, Ltd., Oxford, p. 191.
Hoeksema, J. T., Wilcox, J. M., and Scherrer, P. H.: 1982, *J. Geophys. Res.* **87,** 10 3111.
Howard, R. A. and Koomen, M. J.: 1974, *Solar Phys.* **37,** 469.
Hundhausen, A. J.: 1977, in J. B. Zirker (ed.), *Coronal Holes and High Speed Wind Streams*, Colorado Associated University Press, Boulder, Colorado, p. 225.
Kundt, W.: 1993, in F. Krause, K.-H. Radler, and G. Rüdiger (eds.), *The Cosmic Dynamo*, Kluwer Academic Publishers, Dordrecht, The Netherlands, p. 77.
Legrand, J. P. and Simon, P. A.: 1991, *Solar Phys.* **131,** 187.
Leroy, J. L. and Noens, J. C.: 1983, *Astron. Astrophys.* **120,** L1.
Makarov, V. I. and Sivaraman, K. R.: 1989, *Solar Phys.* **123,** 367.
Mansurov, S. M. and Mansurova, L. G.: 1970, *Ann. Geophys.* **26,** 397.
Mayaud, P. N.: 1980, *Geophysical Monograph Series*, Vol. 22, AGU, Washington, D.C..

Page, D. E.: 1983, in in B. M. McCormac (ed.), *Weather and Climate Responses to Solar Variations*, Colorado Associated University Press, Boulder, CO, p. 345.
Rabiner, L. R. and Gold, B.: 1975, *Theory and Application of Digital Signal Processing*, Prentice-Hall, Inc., Englewood Cliffs, New Jersey.
Richardson, J. D., Paularena, K. I., Belcher, J. W., and Lazarus, A. J.: 1994, *Geophys. Res. Letters* **21,** 1559.
Rybanský, M., Rušin, V., Gaspar, P., and Altrock, R. C.: 1994a, *Solar Phys.* **152,** 487.
Rybanský, M., Rušin, V., Minarovjech, M., and Gaspar, P.: 1994b, *Solar Phys.* **152,** 153.
Sakurai, K.: 1987, in S.-I. Akasofu and Y. Kamide (eds.), *The Solar Wind and the Earth*, Terra Scientific Publishing Co., Tokyo, p. 39.
Simon, P. A. and Legrand, J. P.: 1992, *Solar Phys.* **141,** 391.
Slavin, J. A., Jungman, G., and Smith, E. J.: 1986, *Geophys. Res. Letters* **13,** 513.
Smith, C. W. and Bieber, J. W.: 1996, in D. Winterhalter et al. (eds.), *Solar Wind Eight*, AIP Press, Woodbury, NY, p. 498.
Sonett, C. P.: 1983, in B. M. McCormac (ed.), *Weather and Climate Responses to Solar Variations*, Colorado Associated University Press, Boulder, p. 607.
Sonett, C. P., Webb, G. M., Zakharian, A.: 1997, in J. R. Jokipii, C. P. Sonett, M. S. Giampapa (eds.), *Cosmic Winds and the Heliosphere*, University of Arizona Press, Tucson, p 67.
Stearns, S. D. and David, R. A.: 1988, *Signal Processing Algorithms*, Prentice-Hall, Inc., Englewood Cliffs, New Jersey.
Stenflo, J. O. and Vogel, M.: 1986, *Nature* **319,** 285.
Stern, D.: 1962, *J. Geophys. Res.* **67,** 2133.
Storini, M., Pase, S., Sýkora, J., and Parisi, M.: 1997, *Solar Phys.* **172,** 317.
Stuiver, M.: 1993, *Radiocarbon*, **35**, 67.
Svalgaard, L.: 1972, *Geophysical Papers, R-29*, Charlottenlund, Danish Meteorological Institute, p. 1.
Vennerstrom, S. and Friis-Christensen, E.: 1996, *J. Geophys. Res.* **101,** 24727.
Waldmeier, M: 1961, *The Sunspot-Activity in the Years 1610–1960*, Schulthess, Zürich.
Wang, Y. M. and Sheeley, N. R. Jr.: 1994, *J. Geophys. Res.* **99,** 6597.
Webb, D. F., Davis, J. M., and McIntosh, P. S.: 1984, *Solar Phys.* **92,** 109.
Wilcox, J. M. and Colburn, D. S.: 1972, *J. Geophys. Res.* **77,** 751.
Wilcox, J. M. and Scherrer, P. H.: 1972, *J. Geophys. Res.* **77,** 5385.
Wilcox, J. M. and Svalgaard, L.: 1974, *Solar Phys.* **34,** 461.
Wilcox, J. M., Scherrer, P. H., and Hoeksema, J. T.: 1983, in B. M. McCormac (ed.), *Weather and Climate Responses to Solar Variations*, Colorado Associated University Press, Boulder, CO, p. 365.
Wilson, P. R.: 1994, *Solar and Stellar Activity Cycles*, Cambridge University Press, Cambridge, England.
Wilson, P. R., Altrock, R. C., Harvey, K. L., Martin, S. F., and Snodgrass, H. B.: 1988, *Nature* **333,** 748.
Yoshida, S., Ogita, N., and Akasofu, S. I.: 1971, *J. Geophys. Res.* **76,** 7801.
Yukutake, T. and Cain, J. C.: 1987, *J. Geomagn. Geoelect.* **39,** 19.